Published in final edited form as:
Neurobiol Dis. 2011 September ; 43(3): 543–551. doi:10.1016/j.nbd.2011.04.025.

Decreased glutathione accelerates neurological deficit and mitochondrial pathology in familial ALS-linked hSOD1^{G93A} mice model

Marcelo R. Vargas[1], **Delinda A. Johnson**[1], and **Jeffrey A. Johnson**[1,2,3,4]

[1]Division of Pharmaceutical Sciences, University of Wisconsin, Madison, WI, USA.

[2]Waisman Center, University of Wisconsin, Madison, WI, USA.

[3]Molecular and Environmental Toxicology Center, University of Wisconsin, Madison, WI, USA.

[4]Center for Neuroscience, University of Wisconsin, Madison, WI, USA.

Abstract

Dominant mutations in Cu/Zn-superoxide dismutase (SOD1) cause familial forms of amyotrophic lateral sclerosis (ALS), a fatal disorder characterized by the progressive loss of motor neurons. To investigate the role of antioxidant defenses in ALS we used knockout mice for the glutamate-cysteine ligase modifier subunit (GCLM-/-), which have a 70-80% reduction in total glutathione. Although GCLM(-/-) mice are viable and fertile, the life span of GCLM(-/-)/hSOD1^{G93A} mice decreased in 55% when compared to GCLM(+/+)/hSOD1^{G93A} mice. Decreased life span in GCLM(-/-)/hSOD1^{G93A} mice was associated to increased oxidative stress, aggravated mitochondrial pathology and increased association of hSOD1 with the mitochondria. Interestingly, when the GCLM(-/-) animals were mated with a different ALS-model which overexpress the experimental mutation hSOD1$^{H46R/H48Q}$, no effect was observed in survival of GCLM(-/-)/ hSOD1$^{H46R/H48Q}$ mice; and little or no mitochondrial pathology was observed. Since a specific disease modifier, such as glutathione deficiency, may affect only certain hSOD1 mutants, these findings contribute to our understanding of the potential difference in the molecular pathways by which different hSOD1 mutants generate disease.

Keywords

amyotrophic lateral sclerosis; glutathione; GCLM; mitochondria

Introduction

The tripeptide glutathione (GSH, γ-l-glutamyl-l-cysteinyl-glycine) is the main non-protein thiol found in most aerobics cells. Glutathione serves several physiological functions including: i) direct quenching of radicals, ii) provides reducing equivalents for enzyme-mediated degradation of hydrogen peroxide and organic hydroperoxides, iii) maintenance of

Corresponding author: Jeffrey A. Johnson, Ph.D. School of Pharmacy 6125 Rennebohm Hall Telephone: (608) 262-2893 Fax: (608) 262-5345 jajohnson@pharmacy.wisc.edu.

proteins thiols groups, iv) detoxification of electrophilic xenobiotics, v) provides a reservoir for cysteine and vi) modulates critical cellular process such as DNA synthesis (Meister, 1998). These functions critically affect cell survival under normal or pathological conditions.

Amyotrophic lateral sclerosis (ALS) is the most common adult-onset motor neuron disease, caused by the progressive degeneration of motor neurons in the spinal cord, brain stem, and motor cortex. Motor neuron death leads to muscle weakness and paralysis causing death in one to five years from the time of symptom onset (Rowland and Shneider, 2001). Approximately 10%–20% of familial ALS is caused by a toxic gain-of-function induced by mutations of the Cu/Zn-superoxide dismutase (SOD1) (Rosen et al., 1993). Over 150 mutations in the SOD1 gene have been identified in familial ALS (Turner and Talbot, 2008). Rodents overexpressing mutated forms of hSOD1 generally develop an ALS-like phenotype (Gurney et al., 1994; Howland et al., 2002). Several hypotheses, including oxidative stress, glutamate excitotoxicity, formation of high molecular weight aggregates, and mitochondrial dysfunction have been proposed to explain the toxic effect of mutant SOD1 (Beckman et al., 2001; Cleveland and Rothstein, 2001; Bruijn et al., 2004; Manfredi and Xu, 2005).

Changes in glutathione levels may directly or indirectly aggravate many of the above pathological mechanisms. However, direct evidence of altered glutathione or glutathione utilizing enzymes levels in sporadic and familial ALS remain controversial. For example, while some studies found altered glutathione peroxidase activity others did not (Przedborski et al., 1996a, 1996b; Fujita et al., 1996; Andersen et al., 1998; Kato et al., 2005). In addition, we have shown that activation of Nrf2 reverts the toxicity of astrocytes expressing ALS-linked mutant hSOD1 to co-cultured motor neurons by increasing glutathione production and secretion (Vargas et al., 2006, 2008). Glutathione is synthesized by the consecutive action of two enzymes, glutamate-cysteine ligase (GCL) and glutathione synthetase. The formation of γ-glutamylcysteine by GCL is the rate-limiting reaction in glutathione synthesis and is feedback inhibited by glutathione itself, a mechanism responsible for the regulation of cellular glutathione concentration. GCL is a heterodimer composed of a catalytic subunit (GCLC) and a modifier subunit (GCLM). To further explore the role of glutathione in ALS we have used knockout (KO) mice for GCLM (Yang et al., 2002). Although, the lack of GCLC is lethal, KO mice for GCLM are viable and total glutathione content in different tissues is reduced by 70-80% compared to wild-type littermates. We found that the lack of GCLM significantly accelerates disease and mitochondrial pathology in hSOD1^{G93A} mice, while it does not affect disease presentation in hSOD1$^{H46R/H48Q}$ mice.

Materials and methods

Animals

B6SJL-Tg(SOD1-G93A)1Gur/J (Gurney et al., 1994) were obtained form The Jackson Laboratory (Bar Harbor, ME) and the colony maintained by breeding with B6SJLF1/J females. Male C57BL/6J-GCLM (+/-) mice (Yang et al., 2002) were backcrossed 6 generations to B6SJLF1/J females. Male hSOD1$^{H46R/H48Q}$ mice, originally in a mixed C3H/HeJxC57BL/6J background (Wang et al., 2002) were backcrossed to B6SJLF1/J females for 10 generations to obtain a B6SJL background. GCLM(-/-)/hSOD1^{+} mice were produced by mating F1-GCLM(+/-)/hSOD1^{+} males with F1-GCLM(+/-)/NonTG females. For survival and onset experiments, double transgenic animals were always compared with their contemporaneously produced hSOD1^{G93A} or hSOD1$^{H46R/H48Q}$ littermates. The survival data in Figure 2 correspond to 5♂/8♀ GCLM(+/+)/hSOD1^{G93A}, 9♂/8♀GCLM(+/-)/hSOD1^{G93A} and 4♂/3♀ GCLM(-/-)/hSOD1^{G93A}. The onset data in Figure 2 correspond to 3♂/7♀ GCLM(+/+)/hSOD1^{G93A}, 6♂/3♀ GCLM(+/-)/hSOD1^{G93A} and 3♂/2♀ GCLM(-/-)/hSOD1^{G93A}. The survival data in Figure 6 correspond to 7♂/5♀ GCLM(+/+)/

hSOD1$^{H46R/H48Q}$, 3♂/11♀ GCLM(+/-)/hSOD1$^{H46R/H48Q}$ and 4♂/5♀ GCLM(-/-)/hSOD1$^{H46R/H48Q}$. End-stage was determined by the inability of the animal to right itself within 20 seconds when placed on its side. Mice were weighed three times per week and disease onset was retrospectively determined as the time when mice reached peak body weight. All animal procedures comply with Animal Care and Use Committee requirements of the University of Wisconsin-Madison.

Cell cultures

Primary astrocyte cultures were prepared from spinal cords of 1-day-old mice as previously described (Vargas et al., 2006). Astrocytes were plated at a density of 2×10^4 cells/cm^2 in 35-mm Petri dishes or 24-well plates and maintained in Dulbecco's modified Eagle's medium supplemented with 10% fetal bovine serum, HEPES (3.6 g/L), penicillin (100 IU/mL) and streptomycin (100 μg/mL). Astrocyte monolayers were >98% pure as determined by GFAP immunoreactivity and devoid of OX42-positive microglial cells. Motor neuron cultures were prepared from 12.5 embryonic day mouse spinal cord by an Optiprep-gradient centrifugation (Vargas et al., 2006).

Glutathione and carbonyls measurement

Total glutathione levels (GSH and GSSG) were determined using the Tietze method as previously described (Vargas et al., 2006). Cells were lysed with ice-cold 3% perchloric acid while tissues were lysed in 5 volumes of 5% sulfosalicylic acid. Glutathione content was corrected by protein concentration determined by BCA protein assay (Thermo Scientific, Rockford, IL). GSH content in motor neurons was estimated with monochlorobimane as previously described (Pehar et al., 2007); motor neurons maintained with GDNF (0.1 ng/ml), BDNF (1 ng/ml) and CNTF (10 ng/ml) were incubated for 30 min with monochlorobimane (10 μM) and fixed in ice-cold 4% paraformaldehyde, 0.1% glutaraldehyde in PBS. Fluorescence was imaged immediately after fixing.

To determine GSH:GSSG ratios, reduced (GSH) and oxidized (GSSG) glutathione was measured by normal-phase (ion exchange) HPLC (Fariss and Reed, 1987). Supernatants were alkylated with iodoacetic acid followed by derivatization with 1-flouro-2,4, dinitrobenzene (DNB). The S-carboxymethyl-N-dinitrophenyl-derivatized samples were then loaded onto a 3-aminopropyl-Spherisorb column (Waters Corporation, Milford, MA) and separated by a sodium acetate/methanol gradient using a Shimadzu Prominence HPLC system. Resolved GSH- and GSSG-analyte was detected at 365 nm using a Shimadzu Prominence SPD-20A UV/Vis detector. GSH and GSSG concentrations in the samples were determined by reference GSH and GSSG standard curves included in each run and subsequently normalized to respective tissue protein concentrations.

To determine protein carbonyls, lumbar spinal cord sections were lysed in 20 mM sodium phosphate (pH 6.5), 1mM EDTA plus 1X complete protease inhibitor cocktail-EDTA free (Roche, Indianapolis, IN). Following incubation with streptomycin (1% final concentration) for 15 min at room temperature (RT), samples were centrifuged at 10.000g for 15 min and carbonyls content was assayed with 2,4-dinitrophenylhydrazine using the protein carbonyl assay kit (Cayman, Ann Arbor, MI).

Immunofluorescence and histochemistry

Mice were transcardially perfused with 0.1 M PBS, followed by 4% paraformaldehyde in PBS (pH7.4). Spinal cords were removed, dehydrated, and paraffin embedded. Antigen retrieval was performed in a microwave oven in 0.01 M sodium citrate (pH 6.0) and serial 5μm sections were stained with anti-GFAP (1:500, Dako, Denmark) or anti-Mac2 (1:250, Cedarlane, Canada). All sections were permeabilized with 0.1% Triton X-100 in PBS and

non-specific binding was blocked with 10% goat serum, 2% bovine serum albumin, 0.1% Triton X-100 diluted in PBS for 1 h at RT. Sections were incubated with primary antibodies diluted in blocking solution overnight at 4 °C. Secondary antibodies diluted in blocking solution were incubated for 1 h at RT. Sections were mounted with Fluoro-Gel (EMS, Hatfield, PA). Controls were performed replacing the primary antibody with pre-immune IgG or serum. Secondary antibodies were Alexa Fluor 594-conjugated goat anti-rabbit and Alexa Fluor 488-conjugated goat anti-rat (5μg/ml each, Invitrogen, Carlsbad, CA). Sections were analyzed in an Axiovert microscope (Zeiss, Germany) with Axiovision 4.6 image software.

Motor neuron numbers were determined in 10μm serial sections across the lumbar spinal cord stained with cresyl violet. A blinded independent observer counted every fifth section and a total of 32 sections per animal were analyzed.

For motor root morphology, cross sections were stained overnight with 0.1% luxol fast blue, rinsed in 95% ethanol and water followed by differentiation in lithium carbonate for 10 seconds.

Electron microscopy

Animals were perfused and samples were post-fixed for 2 hs in 2.5% glutaraldehyde, 2.0% paraformaldehyde buffered in 0.1 M sodium phosphate buffer (PB) at RT. The primary fixed samples were rinsed 5 times for 5 minutes in PB, and post-fixed in 1% osmium tetroxide, 1% potassium ferrocyanide in 0.1 M PB for 1 h at RT, and then rinsed in PB as before. Fully dehydrated samples were infiltrated in increasing concentrations of PolyBed 812 (Polysciences Inc. Warrington, PA) and propylene oxide mixtures. The samples were sectioned on a Leica EM UC6 ultramicrotome at 90nm. The sections were collected on Cu, pioloform coated 2×1 oval slot grids (EMS Hatfield, PA), and post-stained in uranyl acetate and lead citrate. The sectioned samples were viewed at 80kV on a Philips CM120 transmission electron microscope, equipped with MegaView III camera (Olympus Soft Imaging System Lakewood, CO).

Western blot analysis

Protein samples (20μg from spinal cords or 5μg from mitochondrial fraction) were resolved on sodium dodecyl sulfate–polyacrylamide gels and transferred to Hybond-P membranes (Amersham, Pittsburgh, PA). Membranes were blocked for 1h in Tris-buffered saline, 0.1% Tween-20 and 5% non-fat dry milk, followed by an overnight incubation with primary antibody diluted in the same buffer. After washing with 0.1% Tween in Tris-buffered saline, the membranes were incubated with peroxidase-conjugated secondary antibody (Amersham) for 1h, and then washed and developed using the ECL chemiluminescent detection system (Amersham). Primary antibodies were rabbit anti-hSOD1 (clone EPR1726, Epitomics, CA), mouse anti-COXI (clone 1D6, Invitrogen) mouse anti-COX5b (clone 16H12, Invitrogen) and mouse anti-complex I subunit NDUFB8 (Mitosciences, Eugene, OR). Densitometric analyses were performed using the NIH Image program and normalized against the signal obtained by reprobing the membranes with anti-actin (Sigma-Aldrich) or anti-VDAC (abcam, Cambridge, MA).

Differential detergent extraction and centrifugation was performed as previously described (Wang et al., 2003) and after the final resuspension, 20μg of protein were assayed for hSOD1 as described above.

Mitochondrial isolation and complex IV activity

Mitochondria were isolated from spinal cords by differential centrifugation using a mitochondria isolation kit for tissue (Thermo Scientific). The mitochondrial fraction typically contained about 1% of the total initial lactate dehydrogenase (LDH) activity (a cytosolic marker). Part of the sample was used immediately to measure Complex IV (cytochrome C oxidase, COX) activity and the rest was used to determine protein concentration and western blot analyses. COX activity was determined by the decrease in absorbance at 550 nm due to the oxidation of reduced cytochrome C by COX. Samples were diluted in 10 mM Tris-HCl pH 7.0, 250 mM sucrose, 1mM n-Dodecyl β-D-maltoside. The reaction buffer included 10 mM Tris-HCl pH 7.0, 120 mM KCl and 10 μM reduced cytochrome C. COX activity was corrected by protein concentration.

Statistical analysis

Each experiment was performed in duplicate and repeated at least three times. Groups of at least three animals were used for biochemical analysis and all data are reported as mean ± SD. Survival and onset data was analyzed with Kaplan-Meier curves and log rank test. Multiple group comparison was performed by one-way ANOVA with Bonferroni's post-test and differences were declared statistically significant if $p < 0.05$. All statistical computations were performed using GraphPad Prism 4.0 (GraphPad Software, San Diego, CA).

Results

Decreased glutathione content in GCLM(-/-) mice

To investigate the effect of decreased glutathione levels in ALS animal models we used KO mice for the modifier subunit of the glutamate-cysteine ligase (GCLM, Yang et al., 2002). Homozygous KO mice for GCLM are viable and appear overtly healthy up to 18 months of age. Total glutathione content in different regions of the central nervous system (CNS) is reduced by 70-80% compared to wild-type littermates. The presence of $hSOD1^{G93A}$ did not alter total glutathione content (Fig. 1A). In addition, no differences in spinal cord reduced/oxidized glutathione (GSH/GSSG) ratio were observed [GCLM(+/+)/NonTG, 61±6; GCLM(+/+)/$hSOD1^{G93A}$, 68±5; GCLM(-/-)/NonTG, 69±7; GCLM(-/-)/$hSOD1^{G93A}$, 58±9]. The decrease in total glutathione is also accompanied by a decrease in mitochondrial glutathione. Specifically, total glutathione content in GCLM(-/-) spinal cord mitochondria is reduced in about 80% (104.2±38.9 pmol/mg prot.) compared to GCLM(+/+) spinal cord mitochondria (499.4±80.5 pmol/mg prot.). The reduction in total glutathione content is also obvious at cell specific level in primary cultures of spinal cord astrocytes (Fig. 1B) and motor neurons (Fig. 1C). Hence, this is an ideal model to study the effect of glutathione deficiency in neurodegeneration.

Lack of GCLM decreased survival in $hSOD1^{G93A}$ mice

We mated the GCLM(-/-) mice to animals overexpressing $hSOD1^{G93A}$ and found that the life span of GCLM(-/-)/$hSOD1^{G93A}$ mice decreased 55% (from 136 days to 59 days) when compared to GCLM(+/+)/$hSOD1^{G93A}$ animals (Fig. 2A). The median onset of symptoms shifted from 104 days in the GCLM(+/+)/$hSOD1^{G93A}$ group to 37 days in GCLM(-/-)/$hSOD1^{G93A}$ mice (Fig. 2B). In this group of animals, disease duration was significantly reduced from 37±6 days in GCLM(+/+)/$hSOD1^{G93A}$ to 20±5 days in GCLM(-/-)/$hSOD1^{G93A}$ mice ($p < 0.05$). Although, there is a significant decrease in brain stem and spinal cord glutathione content in GCLM(+/-) mice (aprox. 20-30%) (Fig. 1A), no effect was observed on survival or disease onset in GCLM(+/-)/$hSOD1^{G93A}$ mice (Fig. 2A, B), suggesting that a critical threshold needs to be reached in order to affect motor neuron survival. When analyzed in 21 days old animals, GCLM(-/-)/$hSOD1^{G93A}$ mice had no

difference in the number of spinal cord motor neurons or the levels of hSOD1^{G93A} expression compared to GCLM(+/+)/hSOD1^{G93A} animals (Fig. 2C, D). The typical glial reaction that accompanies motor neuron degeneration in ALS was also accelerated in GCLM(-/-)/hSOD1^{G93A} mice, and astrocyte reactivity was evident in 30 days old animals (Fig. 3A). Activation of astrocytes and microglia was prominent in terminal (55 days old) GCLM(-/-)/hSOD1^{G93A} animals (Fig. 3A). The gliosis observed on the GCLM(-/-) background was similar to that seen in late stage hSOD1^{G93A} animals in GCLM(+/+) and (+/-) backgrounds (Fig. 3B). In addition, a significant decrease in the number of large neurons in the ventral horn and of lumbar spinal cord root axons was observed in terminal GCLM(-/-)/hSOD1^{G93A} mice when compared to age-matched GCLM(+/+)/hSOD1^{G93A} mice (Fig. 3C, D, E).

Lack of GCLM altered mitochondrial morphology and function in hSOD1^{G93A} mice

We found increased levels of oxidative stress in the spinal cord of terminal GCLM(-/-)/hSOD1^{G93A} mice, as reflected by increased protein carbonyls content (Fig. 4A). Because glutathione is a key component of the mitochondrial antioxidant defenses and mitochondria seem to be an early target in ALS pathogenesis, we investigated mitochondrial morphology and function in GCLM(-/-)/hSOD1^{G93A} mice. Alterations in mitochondrial morphology were evident in neurons from the ventral horn of the spinal cord from asymptomatic (30 days old) and terminal (55 days old) GCLM(-/-)/hSOD1^{G93A} mice (Fig. 4B). In terminal animals, vacuoles in the perikarya appeared to contain mitochondria and/or to be originated from swollen mitochondria (Fig. 4B bottom panel). In addition, the lack of GCLM caused a 3-fold increase in the amount of hSOD1^{G93A} associated with mitochondria isolated from the spinal cord of symptomatic GCLM(-/-)/hSOD1^{G93A} mice compared to age-matched GCLM(+/+)/hSOD1^{G93A} mice (Fig. 4C). The mitochondrial fraction typically contained less than 1% of the total initial lactate dehydrogenase (LDH) activity (a cytosolic marker), indicating that the mitochondrial preparation is mainly free of cytosolic contaminants. Because increased mitochondrial localization of mutant hSOD1 has been associated with decreased complex IV activity (Son et al., 2008), we measured cytochrome c oxidase activity in symptomatic GCLM(-/-)/hSOD1^{G93A} and control mice. The alterations in mitochondrial morphology in GCLM(-/-)/hSOD1^{G93A} mice were accompanied by decreased complex IV (cytochrome c oxidase) activity (Fig. 5A). In turn, decreased complex IV activity correlated with a significant decrease in the levels of two complex IV structural subunits (Fig. 5B, C). Quantitative analysis revealed a ~40% reduction in CIV-subunit I and CIV-subunit Vb levels in GCLM(-/-)/hSOD1^{G93A} when compared to age-matched controls.

Lack of GCLM did not alter survival in hSOD1$^{H46R/H48Q}$ mice

In order to determine if the lack of GCLM, and the associated reduction in total glutathione levels, have a similar effect in other models of hSOD1 overexpression, GCLM(-/-)/hSOD1$^{H46R/H48Q}$ animals were generated. hSOD1$^{H46R/H48Q}$ is a mutant SOD1 that lacks dismutase activity whereas hSOD1^{G93A} is fully active. Unexpectedly, no effect was observed in onset or survival of GCLM(-/-)/hSOD1$^{H46R/H48Q}$ mice compared to GCLM(+/+)/hSOD1$^{H46R/H48Q}$ (Fig. 6A). This differential effect of the decreased glutathione levels on ALS-like pathology in the two transgenic lines was also reflected in that little or no mitochondrial pathology was observed in terminal hSOD1$^{H46R/H48Q}$ mice on either a GCLM(+/+) or GCLM(-/-) background (Fig. 6B). Since there was no difference between the life span of GCLM(+/+)/hSOD1$^{H46R/H48Q}$ and GCLM(-/-)/hSOD1$^{H46R/H48Q}$ mice, we analyzed hSOD1 distribution and mitochondrial function in symptomatic animals of both genotypes. The lack of GCLM did not cause an increase in the amount of hSOD1$^{H46R/H48Q}$ associated with mitochondria isolated from the spinal cord of GCLM(-/-)/hSOD1$^{H46R/H48Q}$ mice compared to age-matched GCLM(+/+)/hSOD1$^{H46R/H48Q}$ mice (Fig. 6C). There was a decrease in complex IV activity associated with hSOD1$^{H46R/H48Q}$ in the GCLM(+/+)

background (Fig 6D; Bar 1 vs. Bar 2). However, this did not correlate with a loss in mitochondrial integrity (Fig. 6B) or reduced levels of complex IV subunits I (Fig. 6E) and Vb (not shown). Interestingly, the GCLM(-/-)/NonTG mice had a comparable significant decrease in complex IV activity relative to GCLM(+/+)/NonTG mice (Fig. 6D; Bar 1 vs. Bar 3). This was independent of $hSOD1^{H46R/H48Q}$ and again did not correlate with a loss in mitochondrial integrity or reduced levels of complex IV subunits. Finally, there was no further decrease in complex IV activity (Fig. 6D; Bar 3 vs. Bar 4) or change in complex IV subunits I (Fig. 6E) and Vb (not shown) in GCLM(-/-)/$hSOD1^{H46R/H48Q}$ mice relative to that observed in the GCLM(-/-)/NonTG mice. In addition, when crossed with mice overexpressing human wild-type SOD1, the survival of GCLM(-/-)/hSOD1WT mice was unaffected during the duration of the above studies (8-9 months).

Discussion

Depletion of glutathione contributes to many pathological conditions (Lu, 2009), however its role in ALS has not been clearly established. Here, we show that the lack of GCLM and the concomitant reduction in total glutathione content significantly impact disease presentation and mitochondrial pathology in $hSOD1^{G93A}$ mice. Although the observation of a 55% decrease in the life span of $hSOD1^{G93A}$ mice in a GCLM-KO background might seem trivial, it has never been reported before and constitutes the first direct *in vivo* evidence for the protective role of glutathione against the neurodegenerative process observed in this ALS-mouse model. In contrast, the lack of GCLM did not affect the survival in a different ALS-mouse model overexpressing the experimental hSOD1 mutation H46R/H48Q.

In principle, decreased glutathione could incorrectly appear to accelerate disease in $hSOD1^{G93A}$ mice if during development alters the baseline number of spinal cord motor neurons. However, no differences were observed among the four groups of animals studied. Therefore, early onset and decreased life span implies that motor neurons were more susceptible to the toxic action of mutant hSOD1. Although we have not rule out the possibility of peripheral pathology, GCLM(-/-)/$hSOD1^{G93A}$ mice displayed a phenotype identical to that observed in GCLM(+/+)/$hSOD1^{G93A}$ mice but with shortened lifespan. Motor symptoms (tremor and loss of extension reflex in hind-limbs, progressive paralysis), muscle wasting (reflected by weight loss), neuronal loss (with axonal degeneration) and gliosis characteristic of late stage GCLM(+/+)/$hSOD1^{G93A}$ mice were obvious in younger GCLM(-/-)/$hSOD1^{G93A}$ mice. In addition to the phenotype and pathological features of the GCLM(-/-)/$hSOD1^{G93A}$ mice, compromised mitochondrial function and morphology in the spinal cord are a strong indication that the absence of GCLM and the associated decrease in glutathione accelerated neurological deficits in $hSOD1^{G93A}$ mice.

Many of the different hypotheses proposed to explain the toxicity of mutant hSOD1 may directly or indirectly be linked to mitochondrial dysfunction and could be affected by the levels of mitochondrial antioxidant capacity. SOD1 is localized predominantly in the cytoplasm, but it is also found in other cellular compartments including the nucleus, endoplasmic reticulum and mitochondria (Crapo et al., 1992; Okado and Fridovich, 2001; Sturtz et al., 2001). The ALS-linked mutant SOD1 proteins have been found in the intermembrane space, matrix or outer membrane of mitochondria from the CNS (Higgins et al., 2002; Vijayvergiya et al., 2005; Vande Velde et al., 2008), but not in peripheral tissues such as muscle and liver (Liu et al, 2004). We found that the lack of GCLM increased the association of $hSOD1^{G93A}$ to spinal cord mitochondria and accelerated mitochondrial morphology and function defects. Mutant hSOD1 found in the mitochondria can display aberrant catalytic chemistry that can damage key mitochondrial enzymes (Beckman et al., 2001), may shift the redox state of respiratory complexes (Ferri et al., 2006) or disrupt the association of cytochrome c with the inner membrane (Kirkinezos et al., 2005). In any of the

above situations, a reduction in mitochondrial antioxidant defenses, caused by decreased glutathione content, may explain the aggravated mitochondrial pathology observed in GCLM(-/-)/hSOD1^{G93A}. Moreover, decreased glutathione content accelerated the disease in GCLM(-/-)/hSOD1^{G93A} mice without increasing the formation of detergent-resistant SOD1 aggregates (data not shown). However, our results do not exclude the possibility that the lack of GCLM aggravates non-mitochondrial hSOD1^{G93A}-mediated toxic mechanisms.

The unexpected observation that the absence of GCLM did not affect disease progression in hSOD1$^{H46R/H48Q}$ mice fosters further discussion of the role of oxidative stress in ALS models bearing mutant forms of hSOD1 that lack SOD activity. Vacuolated, dilated, and disorganized mitochondrial structure occurs in hSOD1^{G93A} and hSOD1^{G37R} mouse models (Dal Canto and Gurney, 1994, Higgins et al., 2003; Kong and Xu, 1998; Wong et al., 1995). However, in hSOD1$^{H46R/H48Q}$ and hSOD1^{G85R} mice, little or no mitochondrial pathology is observed (Wang et al., 2002; Bruijn et al., 1997). Our initial hypothesis was that by reducing glutathione levels, mitochondrial pathology would manifest in hSOD1$^{H46R/H48Q}$. Clearly this was not the case. Although, symptomatic GCLM(+/+)/hSOD1$^{H46R/H48Q}$ and age-matched GCLM(-/-)/hSOD1$^{H46R/H48Q}$ mice displayed decreased complex IV activity relative to non-transgenic mice, no changes in the amount of hSOD1 associated with the mitochondria or reduction in complex IV subunits were detected. These differences may explain, at least in part, the absence of aggravated mitochondrial pathology in terminal GCLM(-/-)/hSOD1$^{H46R/H48Q}$ mice.

hSOD1 mutants differ in important biochemical properties including copper binding, aggregation potential and redox state of an intramolecular disulfide bond that is important in determining the mitochondrial distribution of the enzyme (Son et al., 2007; 2009). In addition, hSOD1 mutants can retain or have no evident SOD activity. hSOD1$^{H46R/H48Q}$ and hSOD1^{G85R} are superoxide dismutase inactive and exist almost exclusively in the reduced form, which may cause the enzyme to localize mainly in the mitochondrial outer membrane (Vande Velde et al., 2008; Son et al., 2009). In contrast, hSOD1^{G93A} retains superoxide dismutase activity, exist in both redox states and is localized in the mitochondrial intermembrane space. Hence, the difference in superoxide dismutase activity or sub-cellular localization of hSOD1 may explain why such a critical modification of the antioxidant defenses (80% reduction in total glutathione content) results in remarkably different observations in two ALS-models. Additional studies will be required to determine if this is a common property shared by other hSOD1 mutants with the above biochemical differences.

Taken together, the current data indicate that glutathione content could be a key disease modifier in ALS by altering mitochondrial function. In particular, because this specific modifier affects only certain hSOD1 mutants, the results obtained may contribute to our understanding of the potential differences in the molecular pathways by which different hSOD1 mutants cause disease. In addition, our data suggest that the value of mitochondria as a viable therapeutic target for ALS needs to be further examined.

Acknowledgments

We thank Dr. Joseph S. Beckman for critical reading of the manuscript and Dr. Timothy Dalton for the GCLM KO mice. In addition, we want to acknowledge Satoshi Kinoshita from the Department of Pathology and Laboratory Medicine as well as Randall Massey from the Medical School Electron Microscope Facility for their technical assistance. This work was supported by grants from the ALS Association and National Institute of Environmental Health Sciences ES08089 (to J.A.J.) and 1K99ES019186 (to M.R.V). M.R.V. was supported in part by the Milton Safenowitz postdoctoral fellowship for ALS research from the ALS Association.

Abbreviations

GCLM-/-	glutamate-cysteine ligase modifier subunit
SOD1	Cu/Znsuperoxide dismutase
ALS	amyotrophic lateral sclerosis
CNS	central nervous system

References

Andersen PM, Nilsson P, Forsgren L, Marklund SL. CuZn-superoxide dismutase, extracellular superoxide dismutase, and glutathione peroxidase in blood from individuals homozygous for Asp90Ala CuZu-superoxide dismutase mutation. J Neurochem. 1998; 70:715–20. [PubMed: 9453566]

Beckman JS, Estevez AG, Crow JP, Barbeito L. Superoxide dismutase and the death of motoneurons in ALS. Trends Neurosci. 2001; 24:S15–S20. [PubMed: 11881740]

Bruijn LI, Becher MW, Lee MK, Anderson KL, Jenkins NA Copeland NG, Sisodia SS, Rothstein JD, Borchelt DR, Price DL, Cleveland DW. ALS-linked SOD1 mutant G85R mediates damage to astrocytes and promotes rapidly progressive disease with SOD1-containing inclusions. Neuron. 1997; 18:327–338. [PubMed: 9052802]

Bruijn LI, Miller TM, Cleveland DW. Unraveling the mechanisms involved in motor neuron degeneration in ALS. Annu Rev Neurosci. 2004; 27:723–749. [PubMed: 15217349]

Cleveland DW, Rothstein JD. From Charcot to Lou Gehrig: deciphering selective motor neuron death in ALS. Nat Rev Neurosci. 2001; 2:806–819. [PubMed: 11715057]

Crapo JD, Oury T, Rabouille C, Slot JW, Chang LY. Copper,zinc superoxide dismutase is primarily a cytosolic protein in human cells. Proc Natl Acad Sci USA. 1992; 89:10405–10409. [PubMed: 1332049]

Dal Canto MC, Gurney ME. Development of central nervous system pathology in a murine transgenic model of human amyotrophic lateral sclerosis. Am J Pathol. 1994; 145:1271–1279. [PubMed: 7992831]

Fariss MW, Reed DJ. High-performance liquid chromatography of thiols and disulfides: dinitrophenol derivatives. Methods Enzymol. 1987; 143:101–119. [PubMed: 3657520]

Ferri A, Cozzolino M, Crosio C, Nencini M, Casciati A, Gralla EB, Rotilio G, Valentine JS, Carrì MT. Familial ALS-superoxide dismutases associate with mitochondria and shift their redox potentials. Proc Natl Acad Sci USA. 2006; 103:13860–13865. [PubMed: 16945901]

Fujita K, Yamauchi M, Shibayama K, Ando M, Honda M, Nagata Y. Decreased cytochrome c oxidase activity but unchanged superoxide dismutase and glutathione peroxidase activities in the spinal cords of patients with amyotrophic lateral sclerosis. J Neurosci Res. 1996; 45:276–281. [PubMed: 8841988]

Gurney ME, Pu H, Chiu AY, Dal Canto MC, Polchow CY, Alexander DD, Caliendo J, Hentati A, Kwon YW, Deng HX. Motor neuron degeneration in mice that express a human Cu,Zn superoxide dismutase mutation. Science. 1994; 264:1772–1775. [PubMed: 8209258]

Higgins CM, Jung C, Xu Z. ALS-associated mutant SOD1G93A causes mitochondrial vacuolation by expansion of the intermembrane space and by involvement of SOD1 aggregation and peroxisomes. BMC Neurosci. 2003; 4:16. [PubMed: 12864925]

Howland DS, Liu J, She Y, Goad B, Maragakis NJ, Kim B, Erickson J, Kulik J, DeVito L, Psaltis G, DeGennaro LJ, Cleveland DW, Rothstein JD. Focal loss of the glutamate transporter EAAT2 in a transgenic rat model of SOD1 mutant-mediated amyotrophic lateral sclerosis (ALS). Proc Natl Acad Sci USA. 2002; 99:1604–1609. [PubMed: 11818550]

Kato S, Kato M, Abe Y, Matsumura T, Nishino T, Aoki M, Itoyama Y, Asayama K, Awaya A, Hirano A, Ohama E. Redox system expression in the motor neurons in amyotrophic lateral sclerosis (ALS): immunohistochemical studies on sporadic ALS, superoxide dismutase 1 (SOD1)-mutated familial ALS, and SOD1-mutated ALS animal models. Acta Neuropathol. 2005; 110:101–112. [PubMed: 15983830]

Kirkinezos IG, Bacman SR, Hernandez D, Oca-Cossio J, Arias LJ, Perez-Pinzon MA, Bradley WG, Moraes CT. Cytochrome c association with the inner mitochondrial membrane is impaired in the CNS of G93A-SOD1 mice. J Neurosci. 2005; 25:164–172. [PubMed: 15634778]

Kong J, Xu Z. Massive mitochondrial degeneration in motor neurons triggers the onset of amyotrophic lateral sclerosis in mice expressing a mutant SOD1. J Neurosci. 1998; 18:3241–3250. [PubMed: 9547233]

Liu J, Lillo C, Jonsson PA, Vande Velde C, Ward CM, Miller TM, Subramaniam JR, Rothstein JD, Marklund S, Andersen PM, Brännström T, Gredal O, Wong PC, Williams DS, Cleveland DW. Toxicity of familial ALS-linked SOD1 mutants from selective recruitment to spinal mitochondria. Neuron. 2004; 43:5–17. [PubMed: 15233913]

Lu SC. Regulation of glutathione synthesis. Mol Aspects Med. 2009; 30:42–59. [PubMed: 18601945]

Manfredi G, Xu Z. Mitochondrial dysfunction and its role in motor neuron degeneration in ALS. Mitochondrion. 2005; 5:77–87. [PubMed: 16050975]

Meister A. Glutathione metabolism and its selective modification. J Biol Chem. 1988; 263:17205–17208. [PubMed: 3053703]

Okado-Matsumoto A, Fridovich I. Subcellular distribution of superoxide dismutases (SOD) in rat liver: Cu,Zn-SOD in mitochondria. J Biol Chem. 2001; 276:38388–38393. [PubMed: 11507097]

Pehar M, Vargas MR, Robinson KM, Cassina P, Díaz-Amarilla PJ, Hagen TM, Radi R, Barbeito L, Beckman JS. Mitochondrial superoxide production and nuclear factor erythroid 2-related factor 2 activation in p75 neurotrophin receptor-induced motor neuron apoptosis. J Neurosci. 2007; 27:7777–7785. [PubMed: 17634371]

Przedborski S, Donaldson D, Jakowec M, Kish SJ, Guttman M, Rosoklija G, Hays AP. Brain superoxide dismutase, catalase, and glutathione peroxidase activities in amyotrophic lateral sclerosis. Ann Neurol. 1996a; 39:158–165. [PubMed: 8967746]

Przedborski S, Donaldson DM, Murphy PL, Hirsch O, Lange D, Naini AB, McKenna-Yasek D, Brown RH Jr. Blood superoxide dismutase, catalase and glutathione peroxidase activities in familial and sporadic amyotrophic lateral sclerosis. Neurodegeneration. 1996b; 5:57–64. [PubMed: 8731383]

Rosen DR, et al. Mutations in Cu/Zn superoxide dismutase gene are associated with familial amyotrophic lateral sclerosis. Nature. 1993; 362:59–62. [PubMed: 8446170]

Rowland LP, Shneider NA. Amyotrophic lateral sclerosis. N Engl J Med. 2001; 344:1688–1700. [PubMed: 11386269]

Son M, Fu Q, Puttaparthi K, Matthews CM, Elliott JL. Redox susceptibility of SOD1 mutants is associated with the differential response to CCS over-expression in vivo. Neurobiol Dis. 2009; 34:155–162. [PubMed: 19320055]

Son M, Puttaparthi K, Kawamata H, Rajendran B, Boyer PJ, Manfredi G, Elliott JL. Overexpression of CCS in G93A-SOD1 mice leads to accelerated neurological deficits with severe mitochondrial pathology. Proc Natl Acad Sci USA. 2007; 104:6072–6077. [PubMed: 17389365]

Sturtz LA, Diekert K, Jensen LT, Lill R, Culotta VC. A fraction of yeast Cu,Znsuperoxide dismutase and its metallochaperone, CCS, localize to the intermembrane space of mitochondria. A physiological role for SOD1 in guarding against mitochondrial oxidative damage. J Biol Chem. 2001; 276:38084–38089. [PubMed: 11500508]

Turner BJ, Talbot K. Transgenics, toxicity and therapeutics in rodent models of mutant SOD1-mediated familial ALS. Prog Neurobiol. 2008; 85:94–134. [PubMed: 18282652]

Vande Velde C, Miller TM, Cashman NR, Cleveland DW. Selective association of misfolded ALS-linked mutant SOD1 with the cytoplasmic face of mitochondria. Proc Natl Acad Sci USA. 2008; 105:4022–4027. [PubMed: 18296640]

Vargas MR, Johnson DA, Sirkis DW, Messing A, Johnson JA. Nrf2 activation in astrocytes protects against neurodegeneration in mouse models of familial amyotrophic lateral sclerosis. J Neurosci. 2008; 28:13574–13581. [PubMed: 19074031]

Vargas MR, Pehar M, Cassina P, Beckman JS, Barbeito L. Increased glutathione biosynthesis by Nrf2 activation in astrocytes prevents p75NTR-dependent motor neuron apoptosis. J Neurochem. 2006; 97:687–696. [PubMed: 16524372]

Vijayvergiya C, Beal MF, Buck J, Manfredi G. Mutant superoxide dismutase 1 forms aggregates in the brain mitochondrial matrix of amyotrophic lateral sclerosis mice. J Neurosci. 2005; 25:2463–2470. [PubMed: 15758154]

Wang J, Slunt H, Gonzales V, Fromholt D, Coonfield M, Copeland NG, Jenkins NA, Borchelt DR. Copper-binding-site-null SOD1 causes ALS in transgenic mice: aggregates of non-native SOD1 delineate a common feature. Hum Mol Genet. 2003; 12:2753–2764. [PubMed: 12966034]

Wang J, Xu G, Gonzales V, Coonfield M, Fromholt D, Copeland NG, Jenkins NA, Borchelt DR. Fibrillar inclusions and motor neuron degeneration in transgenic mice expressing superoxide dismutase 1 with a disrupted copper-binding site. Neurobiol Dis. 2002; 10:128–138. [PubMed: 12127151]

Wong PC, Pardo CA, Borchelt DR, Lee MK, Copeland NG, Jenkins NA, Sisodia SS, Cleveland DW, Price DL. An adverse property of a familial ALS-linked SOD1 mutation causes motor neuron disease characterized by vacuolar degeneration of mitochondria. Neuron. 1995; 14:1105–1116. [PubMed: 7605627]

Yang Y, Dieter MZ, Chen Y, Shertzer HG, Nebert DW, Dalton TP. Initial characterization of the glutamate-cysteine ligase modifier subunit Gclm(-/-) knockout mouse. Novel model system for a severely compromised oxidative stress response. J Biol Chem. 2002; 277:49446–49452. [PubMed: 12384496]

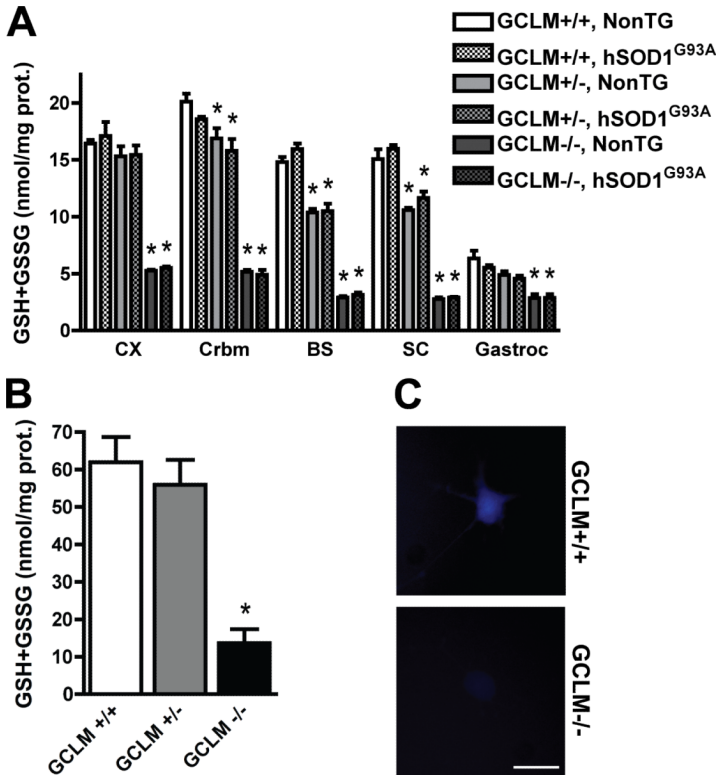

Figure 1.

Decreased total glutathione content in GCLM-/- mice. A) Total glutathione (GSH+GSSG) content in different tissues from 30 days old GCLM(+/+), GCLM(+/-) and GCLM(-/-) mice in the presence or absence of $hSOD1^{G93A}$. CX, Frontal cortex; Crbm, cerebellum; BS, brainstem; SC, spinal cord; Gastroc, gastrocnemius muscle. Each bar represents the mean ± SD, n=3-5. *Significantly different from its respective GCLM(+/+) tissue ($p<0.05$). B) Total glutathione (GSH+GSSG) content in primary GCLM(+/+), GCLM(+/-) and GCLM(-/-) spinal cord astrocyte cultures. Each bar represents the mean±SD, n=5. *Significantly different from GCLM(+/+) ($p<0.05$). C) Microphotographs showing GSH content in primary GCLM(+/+) and GCLM(-/-) motor neurons after 48 hrs in culture as reflected by monochlorobimane fluorescence. Scale bar: 20μm.

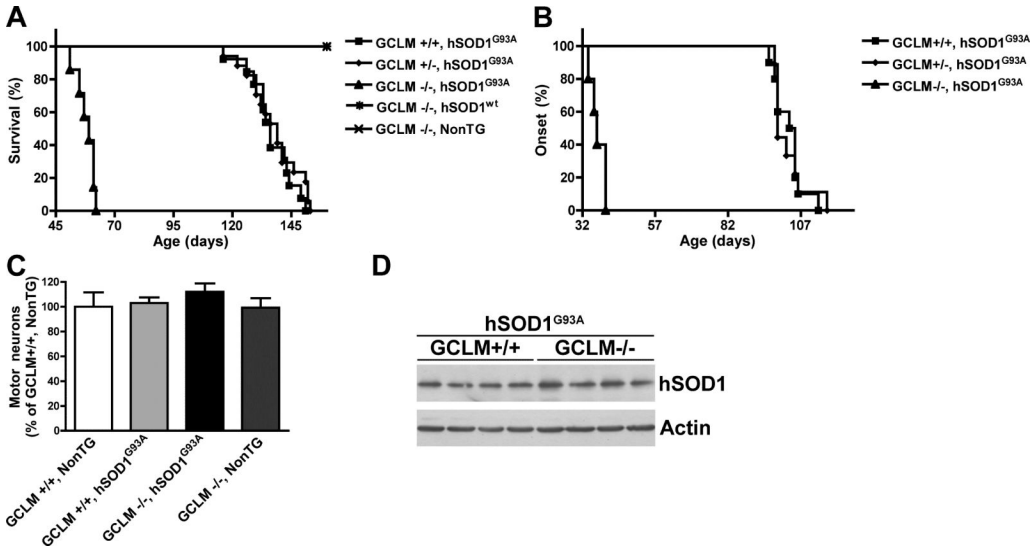

Figure 2.

Decreased glutathione levels reduce survival in hSOD1^{G93A} mice. A) Lack of GCLM decreased the median survival from 136 days in GCLM(+/+)/hSOD1^{G93A} animals (n=13) to 59 days in GCLM(-/-)/hSOD1^{G93A} animals (n=7). Survival curves are significantly different $p<0.0001$ ($\chi 2=54.73$). B) Lack of GCLM decreased the median onset from 104 days in GCLM(+/+)/hSOD1^{G93A} animals (n=10) to 37 days in GCLM(-/-)/hSOD1^{G93A} animals (n=5). Onset curves are significantly different $p<0.0001$ ($\chi 2=26.76$). C) Number of ventral horn motor neurons in the lumbar spinal cord from 21 days old mice of the indicated genotype. Data are presented as percentage of GCLM(+/+)/NonTG animals (mean±SD; n=3). No significant difference was observed among the four groups of mice. D) hSOD1 protein expression in 21 days old spinal cord extracts from GCLM(+/+)/hSOD1^{G93A} and GCLM(-/-)/hSOD1^{G93A} mice. No difference was observed in hSOD1 levels between GCLM(+/+)/hSOD1^{G93A} (100±19; n=4) and GCLM(-/-)/hSOD1^{G93A} (99±22; n=4) mice when quantified and corrected by actin levels.

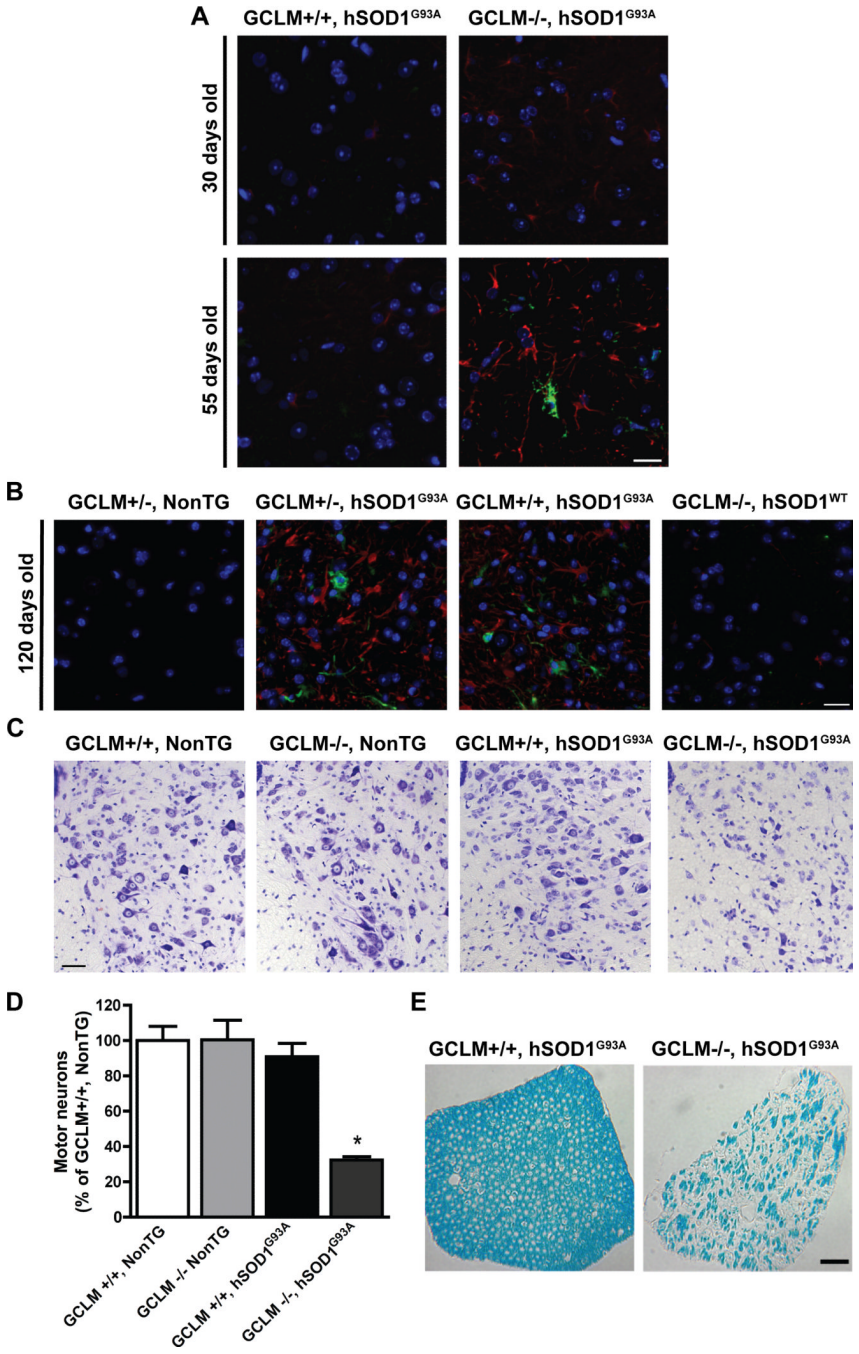

Figure 3.

Astrogliosis and motor neuron loss in GCLM(-/-)/hSOD1^{G93A} mice. A and B) Immunofluorescence against GFAP (red) and Mac2 (green) in the anterior horn of the lumbar spinal cord from 30, 55 and 120 days old mice of the transgenic genotypes indicated in the figure. Nuclei were counterstained with DAPI. Scale bars: 20 μm. C) Representative images from the lumbar ventral horn of terminal (55 days old) GCLM(-/-)/hSOD1^{G93A} and age-matched controls. Scale bar: 40 μm. D) Number of large neurons in the ventral horn of the lumbar spinal cord from 55 days old mice of the indicated genotype. Data are presented as percentage of GCLM(+/+)/NonTG animals (mean±SD; n=3. * $p<0.05$). E) Luxol fast

blue staining in cross sections of lumbar spinal cord roots from terminal (55 days old) GCLM(-/-)/hSOD1^{G93A} and age-matched GCLM(+/+)/hSOD1^{G93A} mice. Scale bar: 50 μm.

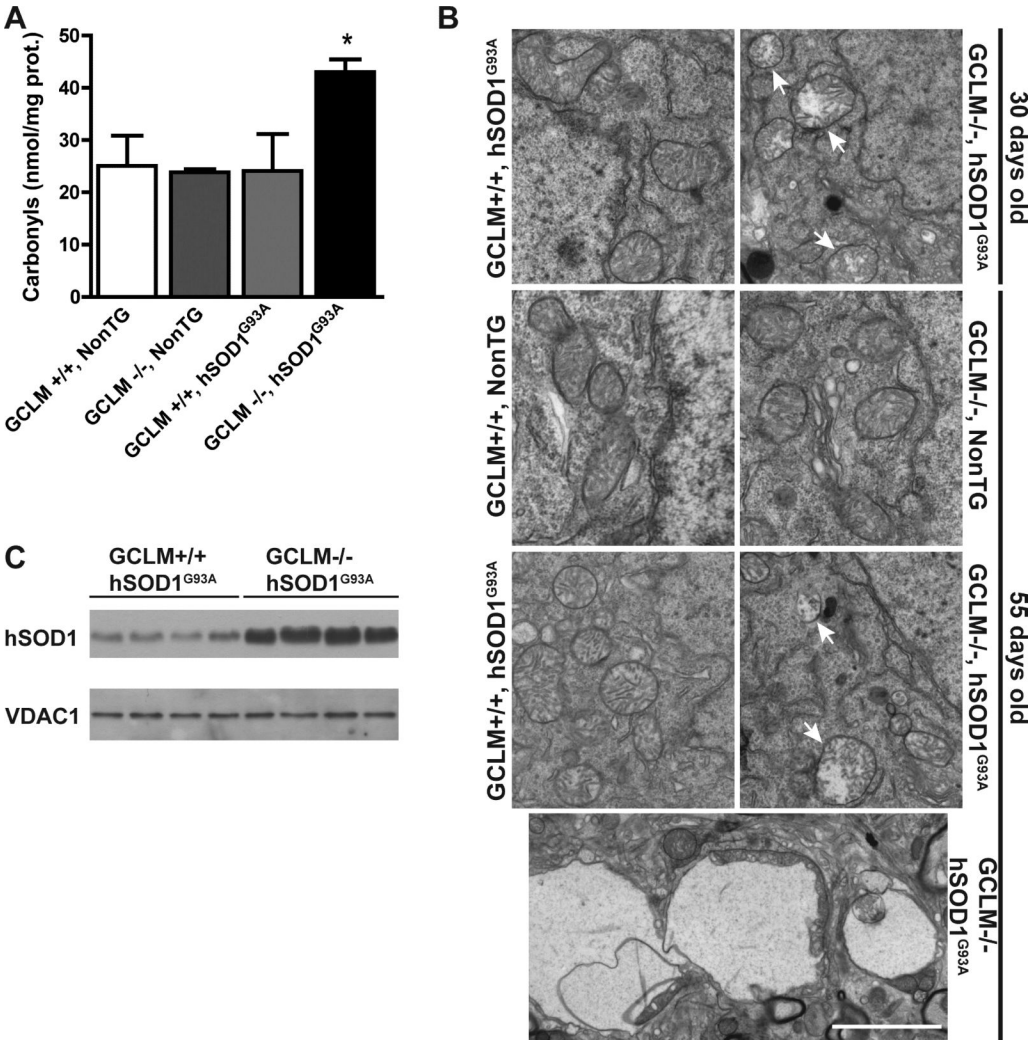

Figure 4.

Increased oxidative stress and altered mitochondrial morphology in the spinal cord of GCLM(-/-)/hSOD1^{G93A} mice. A) Protein carbonyl content in lumbar spinal cord extracts from 55 days old mice of the indicated genotypes. Data are presented as mean±SD; n=3. * $p<0.05$. B) Electron microscopy of neurons from the ventral horn of lumbar spinal cords cord. The top part shows mitochondrial vacuolization in 30 days old GCLM(-/-)/ hSOD1^{G93A} mice. At 55 days, remaining motor neurons in GCLM(-/-)/hSOD1^{G93A} mice also display mitochondrial damage. The bottom panel shows the typical vacuolar degeneration observed in these animals. Arrows denote degenerating mitochondria. Scale bar: 2 μm. C) hSOD1 levels in purified mitochondria from the spinal cord of symptomatic (42 days old) GCLM(-/-)/hSOD1^{G93A} and age-matched GCLM(+/+)/hSOD1^{G93A} mice. There is a significant increase in the amount of hSOD1 associated with the mitochondria of GCLM(-/-)/hSOD1^{G93A} mice (339±69; n=4) compared to GCLM(+/+)/hSOD1^{G93A} mice (100±24; n=4, $p<0.05$), when quantified and corrected by VDAC1 levels.

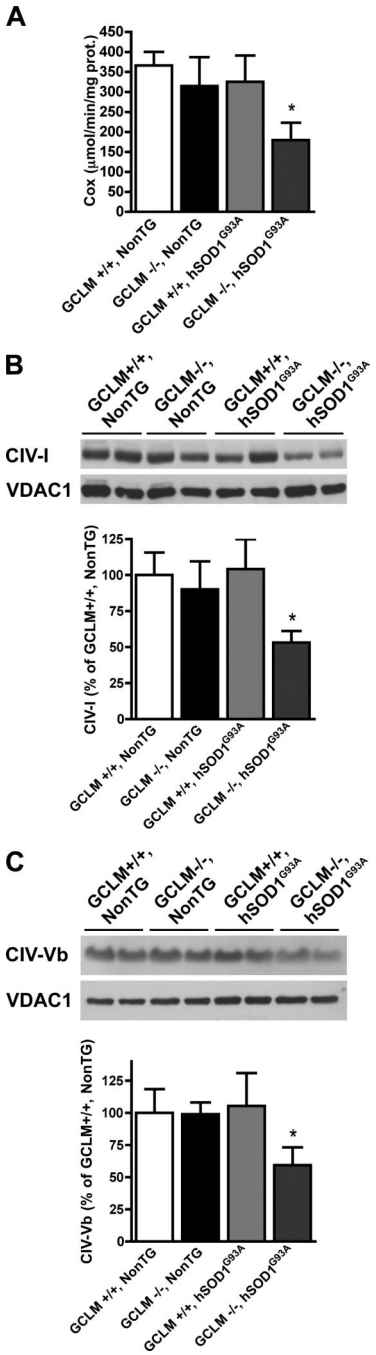

Figure 5.

Decreased mitochondrial complex IV activity and structural subunits expression in the spinal cord of symptomatic GCLM(-/-)/hSOD1^{G93A} mice. A) Complex IV (cytochrome C oxidase, Cox) activity in enriched mitochondria from symptomatic (42 days old) GCLM(-/-)/hSOD1^{G93A} mice and age-matched controls. Each bar represents the mean±SD, n=4. *Significantly different from GCLM(+/+)/NonTG (p<0.05). Levels of complex IV subunit I (B) and subunit Vb (C) in enriched mitochondria fractions from 42 days old mice of the transgenic genotypes indicated in the figure. Protein loading was corrected by VDAC1 levels. Data are expressed as percentage of GCLM(+/+)/NonTG (mean±SD, n=4). *Significantly different from GCLM(+/+)/NonTG (p<0.05).

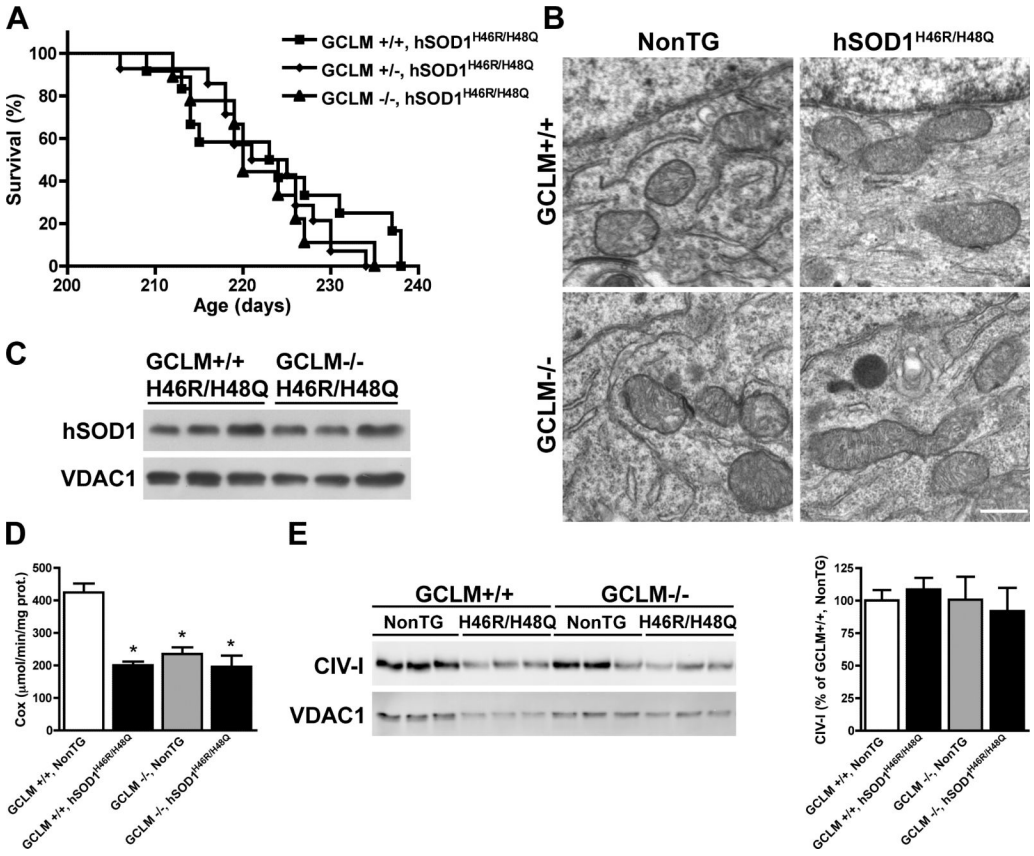

Figure 6.

Reduced glutathione content does not affect the survival and mitochondrial morphology of GCLM(-/-)/hSOD1$^{H46R/H48Q}$ mice. A) No significant difference was observed in the median survival of GCLM(+/+)/hSOD1$^{H46R/H48Q}$ (223.5 days, n=12), GCLM(+/-)/hSOD1$^{H46R/H48Q}$ (223 days, n=14) and GCLM(-/-)/hSOD1$^{H46R/H48Q}$ (220 days, n=9) mice. B) Electron microscopy of lumbar spinal cord motor neurons in terminal animals (>210 days old) of the indicated genotypes. No alterations in mitochondrial morphology was observed in GCLM(-/-)/hSOD1$^{H46R/H48Q}$ mice. Scale bar: 1 μm. C) hSOD1 levels in purified mitochondria from the spinal cord of symptomatic GCLM(-/-)/hSOD1$^{H46R/H48Q}$ and age-matched GCLM(+/+)/hSOD1$^{H46R/H48Q}$ mice. No difference was observed in hSOD1 levels between GCLM(+/+)/hSOD1$^{H46R/H48Q}$ (100±35; n=3) and GCLM(-/-)/hSOD1$^{H46R/H48Q}$ (105±6; n=3) animals, when quantified and corrected by VDAC1 levels. D) Complex IV (cytochrome C oxidase, Cox) activity in enriched mitochondria from symptomatic GCLM(-/-)/hSOD1$^{H46R/H48Q}$ mice and age-matched controls. Each bar represents the mean ±SD, n=6. *Significantly different from GCLM(+/+)/NonTG (p<0.05). E) Levels of complex IV subunit I in enriched mitochondria fractions from symptomatic mice of the indicated genotypes. In the right panel data are expressed as percentage of GCLM(+/+)/NonTG (mean±SD, n=3). No significant difference was observed among the four groups of mice, when quantified and corrected by VDAC1 levels.